References and Notes

1. B. C. Murray *et al. Science* **183**, 1307 (1974).
2. M. J. S. Belton, G. R. Smith, D. A. Elliott, K. Klaasen, G. E. Danielson, *J. Atmos. Sci.* **33**, 1383 (1976); M. J. S. Belton, G. R. Smith, G. Schubert, A. D. Del Genio, *ibid.*, p. 1394.
3. Periods of nearly full-disk imaging will occur from the middle of August to the end of October 1979 and from the beginning of April to the middle of June 1980. Several reasons for anticipating that climate variations will be observable over a time scale of several hundred Earth days are: (i) ground-based ultraviolet images show major global changes on these time scales, such as the appearance or disappearance of a bright cloud covering either polar region (*4*); (ii) ground-based observations of the integrated disk polarization of Venus at 365 nm [figure 17 of (*5*)] show long-term variations in the mean contribution of Rayleigh scattering; (iii) the radiative time scale is tens to hundreds of days at the altitudes of the main clouds of Venus, 45 to 65 km (*6*); (iv) several cloud physics time scales are of the order of 10^7 seconds for particles of the size in the visible clouds of Venus (*7*).
4. A. Dollfus, *J. Atmos. Sci.* **32**, 1060 (1975).
5. D. L. Coffeen and J. E. Hansen, in *Planets, Stars, and Nebulae*, T. Gehrels, Ed. (Univ. of Arizona Press, Tucson, 1974), p. 518.
6. R. M. Goody and M. J. S. Belton, *Planet. Space Sci.* **15**, 247 (1967).
7. W. B. Rossow, *Icarus* **36**, 1 (1978).
8. The OCPP was built by Santa Barbara Research Center under specifications from the Goddard Institute for Space Studies. The instrument is described by E. Russell, L. Watts, S. Pellicori, and D. Coffeen [*Proc. Soc. Photo-Opt. Instrum. Eng.* **112**, 28 (1977)] and by L. Colin and D. M. Hunten [*Space Sci. Rev.* **20**, 451 (1977)].
9. The phase angle is the angle between the sun-planet and planet-observer directions, defined as zero for direct backscattering. The zenith angle is the angle between the local normal to the planetary surface and the direction of the sun (solar zenith angle) or the direction of observation.
10. The polarization as a function of phase angle and wavelength can be used to obtain the size, shape, and refractive index of aerosols. Quantitative discussions are given in (*5*), (*11*), and (*12*).
11. J. E. Hansen and L. D. Travis, *Space Sci. Rev.* **16**, 527 (1974).
12. J. E. Hansen and J. W. Hovenier, *J. Atmos. Sci.* **31**, 1137 (1974); K. Kawabata and J. E. Hansen, *ibid.* **32**, 1133 (1975).
13. The ultraviolet spectrometer has a fixed view direction 60° from the positive z (spin) axis, whereas the infrared radiometer has a fixed view direction of 45°.
14. Identification of OCPP images of Venus is by consecutive numbers in order of acquisition, starting with 1 for the first image acquired on 5 December 1978.
15. The phase angle specified for an image or polarimetry map is the value for disk center at the time the subspacecraft point was observed. Thus, the phase angle for a particular point on the disk at the time it was observed can be different because of the finite distance of the spacecraft from the planet and the finite time employed to acquire the image. The former effect is the larger, giving rise to a maximum difference equal to the angular radius of the planet which ranges from 5° to 9° for the portion of the orbit during which imaging is normally performed.
16. S. S. Limaye and V. E. Suomi, *J. Atmos. Sci.* **34**, 205 (1977).
17. V. E. Suomi and S. S. Limaye, *Science* **201**, 1009 (1978).
18. C. Boyer and P. Guerin, *Icarus* **11**, 338 (1969); R. F. Beebe, *ibid.* **17**, 602 (1972); A. H. Scott and E. J. Reese, *ibid.*, p. 589.
19. The polarization is positive if the intensity in the plane of scattering is smaller than that in the perpendicular plane. Thus, Rayleigh scattering is positive, while light scattered from aerosols may be positive or negative depending on the physical characteristics of the particles [compare with (*11*)].
20. The calculations for Fig. 5 are for spherical particles. Similar calculations of spheroids by S. Asano and M. Sato (personal communication) indicate substantial change only for very nonspherical shapes.
21. The polarization at $\lambda \sim 1$ μm has been anomalous at times; both the current values at 0.935 μm and some previous ground-based values at 0.99 μm [A. Dollfus and D. L. Coffeen, *Astron. Astrophys.* **8**, 251 (1970)] are well above the long-term mean. The polarization in the ultraviolet also shows strong temporal variations (*5*), as does the strength of the rainbow in the polarization at visible and shorter wavelengths. This could be due, for example, to changes in the main cloud or in the amount of blanketing by the stratospheric haze.
22. W. A. Lane, *Astron. J.*, in press; J. V. Martonchik and R. Beer, *J. Atmos. Sci.* **32**, 1151 (1975).

23. We thank the Santa Barbara Research Center for the detailed design, construction, and calibration of the orbiter cloud photopolarimeter, which has performed flawlessly. We are very grateful to R. Fimmel, S. Hing, B. Pittman, and others at the Pioneer Project Office, Ames Research Center, for implementing our command sequences to the OCPP, and W. B. Rossow for his comments on a draft of this paper. D.L.C. and W.A.L. were supported by NASA grant 33-015-165 to State University of New York at Stony Brook. S.S.L. was supported by a National Research Council postdoctoral research associateship.

16 January 1979

Infrared Image of Venus at the Time of Pioneer Venus Probe Encounter

Abstract. *An image of the infrared emission from the Earth-facing hemisphere of Venus was obtained at the time the Pioneer Venus probes penetrated the atmosphere. The thermal structure of the atmosphere at the 85-millibar level included regions of rapidly varying polar features, a solar-related postdawn warm area, and a nonsolar-fixed nighttime warm area. The probes succeeded in entering each of these three thermal regions.*

As part of a program of ground-based thermal observations of Venus designed to characterize the spatial and temporal extent of thermal emissions from the Venus clouds, we obtained a hemisphere-wide infrared view of the planet during the entry of the Pioneer Venus probes. The observations were made with a bolometric detector viewing through a filter with a 10.6- to 12.6-μm spectral pass-

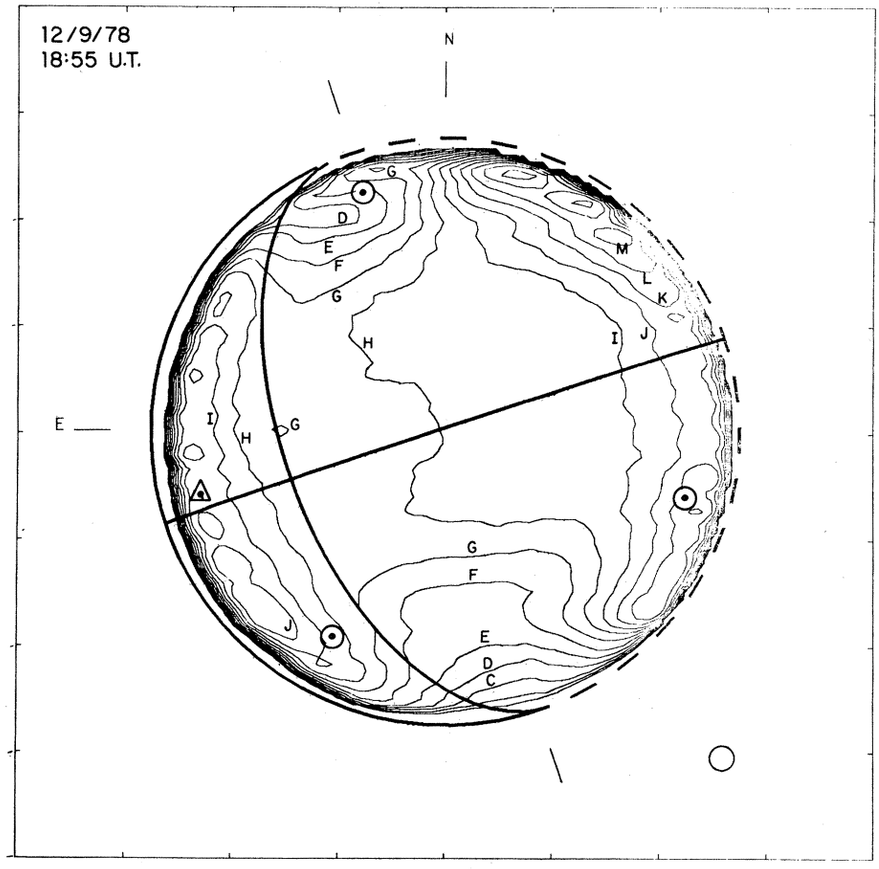

Fig. 1. Isophotal map of infrared emission from Venus at the time of probe entry with limb darkening removed. The radiance contours are equally spaced, by 2 percent of the average central intensity. Entry sites of small probes are indicated by circles, that of the large probe by a triangle. The dawn terminator, equator, and orientation of the Venus pole are shown, as are celestial north and east. The borders of the map enclosed a region measuring 64 by 64 arc seconds; the small circle in the lower right is the size of the detector aperture.

0036-8075/79/0223-0785$00.50/0

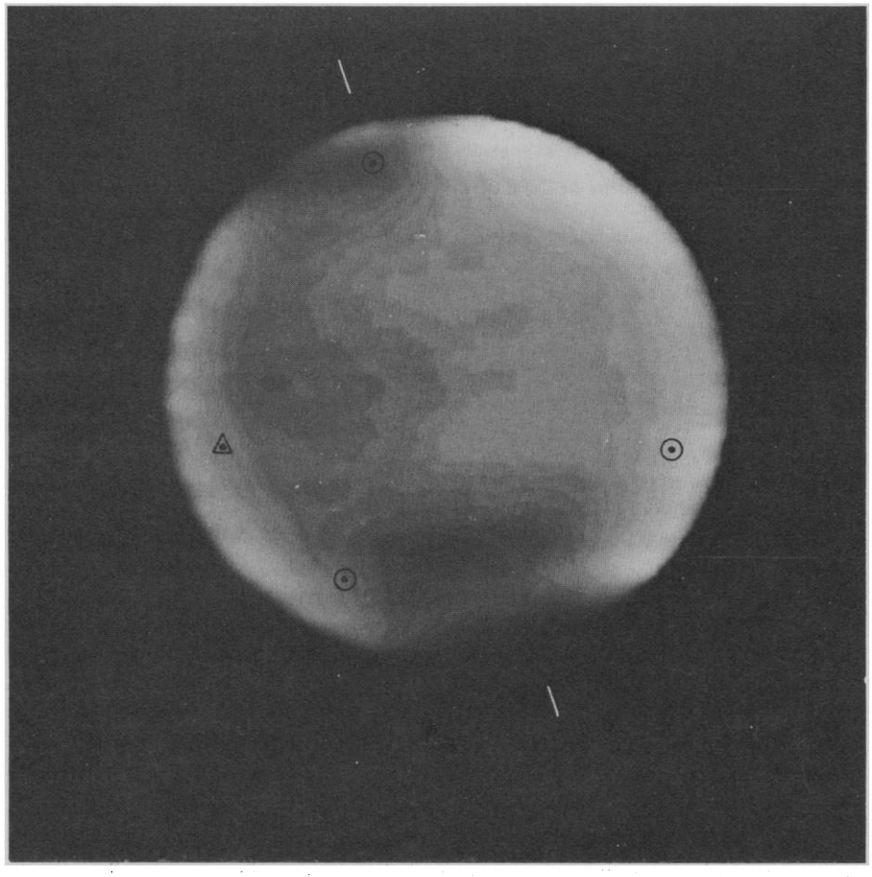

Fig. 2. Gray-tone representation of the radiance map shown in Fig. 1. Black represents the lowest infrared radiance, white the highest. The probe entry sites and orientation of the Venus pole are shown with the same conventions as in Fig. 1.

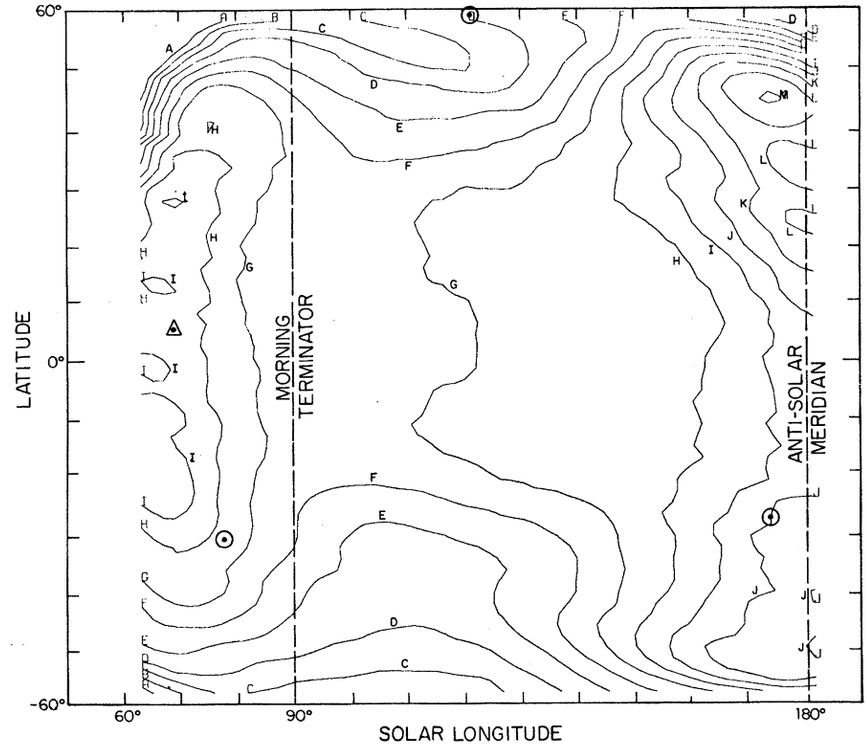

Fig. 3. Mercator projection of the infrared emission into a frame fixed with respect to the sun. Contours are spaced at intervals of 2 percent of the average central intensity; contour *A* represents the lowest infrared radiance and *M* the highest. Small probe entry sites are indicated by circles, the large probe site by a triangle.

band, whose weighting function peaks at the 85-mbar level, approximately 67 km above the surface.

The thermal features of Venus have been observed sporadically since 1964 (*1-3*); the aim of the present program is a systematic characterization of the major thermal features and their changes over both the 14-week observation period during the 1978 conjunction and the 19-month period since our 1977 observations (*4*). The images are built up with the 1.5-m telescope at Mount Hopkins, Arizona, by a raster scanning the image of Venus across the detector aperture, moving the telescope in declination and a small scanning tertiary mirror in right ascension. The spatial resolution is 1.8 arc seconds (Venus appeared 43.8 arc seconds in diameter at the time of the probe entry). Each raster scan of the planet requires 2 minutes, and 32 such scans were taken at the time of probe entry; these scans were processed to remove instrumental effects and added together as described in (*4*).

To enhance the visibility of the weak thermal features, we removed the planet's general limb darkening by dividing the added image by a monotonic function of only μ, the cosine of the viewing angle: this procedure removes the dominant radially symmetrical features.

The added image obtained at the time of probe entry (*5*) is presented as a contour map in Fig. 1 and a gray-tone image in Fig. 2. Normalized relative infrared radiances are shown, with contours spaced at 2 percent of the average central intensity over the central 25 percent of the disk. For temperatures close to 240 K our observed radiances vary as the fifth power of the emission temperature, so that a 2 percent change is equivalent to 1 K. The probe entry sites (at 65 km) are indicated by circles for the small probes and a triangle for the large probe in Fig. 1. Also shown are the location of the rotation axis, the dawn terminator, the planet's equator, and celestial east and north. Black on the image and contour *A* on the map are the areas of lowest infrared radiance, and white and contour *M* the highest. The data are also displayed in a solar-fixed mercator projection in Fig. 3, between 180° and 60° solar longitude (midnight through 8 a.m. local time), with contours spaced at 2 percent intervals.

Two intense polar regions of low emission extended as far south as 37°N in the northern hemisphere and as far north as 26°S in the southern hemisphere. The region near the south pole was relatively symmetrical on 9 December, but the north region showed a plume of very low

emission, sometimes described as a cold ring, extending partly around a plateau of higher emission near the pole itself. This is the first observation of a low-emission region around a warmer plateau near the north pole, probably because of this year's favorable viewing geometry (*6*), although such features have previously been seen near the south pole (*2*, *4*).

The region of highest thermal emission on this day was on the nightside of the planet, at roughly 45°N. This sharply contrasts with the observations we made in April and May 1977 (*4*) at an identical solar phase angle, in which the region of intense emission was consistently on the sunlit side of the terminator. This striking change of appearance indicates that at least some of the major thermal features are not solar-fixed. In addition, since the features observed in 1977 did persist over the 26-day observation period, the time scale for the observed atmospheric thermal change must be on the order of several months, but less than the 19 months separating the observations. A solar component is observable, however, since postdawn infrared brightening begins at roughly 75° solar longitude in both data sets (although the warmest area shifted from north of the equator in May 1977 to somewhat south of the equator on 9 December 1978).

The north probe entered near the boundary of the subpolar cold ring and the warmer polar plateau, well within the region of the polar thermal feature characterized by rapid daily changes (*4*). The site of entry of the night probe was in one of the two well-developed warm regions near the antisolar meridian (the cooler of the two). The day probe entered near the boundary between the cold south polar region and the region of postdawn brightening, but definitely outside the cold polar zone. The large probe entered a stable area in the region of postdawn brightening, which extended roughly homogeneously from 30°N to 30°S latitude. The probes entered at least three distinct types of thermal provinces: the cold ring–warm plateau zone near the north pole, a region of nighttime thermal brightening, and the postdawn warming area. These areas were broadly representative of nearly all the types of thermal features observed on the hemisphere visible from Earth at the time of encounter, and should provide a good characterization of its major dynamical regions.

JEROME APT
RICHARD GOODY
Center for Earth and Planetary Physics, Harvard University, Cambridge, Massachusetts 02138

References and Notes

1. B. C. Murray, R. L. Wildey, J. A. Westphal, *J. Geophys. Res.* **68**, 4813 (1963); J.A. Westphal, R. L. Wildey, B. C. Murray, *Astrophys. J.* **142**, 799 (1965).
2. D. J. Diner, J. A. Westphal, F. P. Schloerb, *Icarus* **27**, 191 (1976).
3. R. A. Brown and R. M. Goody, *ibid.* **35**, 189 (1978).
4. J. Apt and R. Goody, *J. Geophys. Res.*, in press.
5. The observations were centered at 1855 UT on 9 December 1978 (Julian date 2443852.29): the subearth Venus latitude was 0.6°S; subearth Venus longitude, 2.7°; subearth heliocentric longitude, 123.1°.
6. The subearth Venus latitude of 0.6°S was smaller than that during any previous observations and allowed nearly identical viewing geometries for both poles.
7. Supported by NASA contract NAS2-9127 from the Pioneer Project Office.

16 January 1979

Structure of the Atmosphere of Venus up to 110 Kilometers: Preliminary Results from the Four Pioneer Venus Entry Probes

Abstract. *The four Pioneer Venus entry probes transmitted data of good quality on the structure of the atmosphere below the clouds. Contrast of the structure below an altitude of 50 kilometers at four widely separated locations was found to be no more than a few degrees Kelvin, with slightly warmer temperatures at 30° south latitude than at 5° or 60° north. The atmosphere was stably stratified above 15 or 20 kilometers, indicating that the near-adiabatic state is maintained by the general circulation. The profiles move from near-adiabatic toward radiative equilibrium at altitudes above 40 kilometers. There appears to be a region of vertical convection above the dense cloud deck, which lies at 47.5 to 49 kilometers and at temperature levels near 360 K. The atmosphere is nearly isothermal around 100 kilometers (175 to 180 K) and appears to exhibit a sizable temperature wave between 60 and 70 kilometers. This is where the 4-day wind is believed to occur. The temperature wave may be related to some of the wavelike phenomena seen in Mariner 10 ultraviolet photographs.*

Each of the four Pioneer Venus probes carried instruments to measure the structure of the atmosphere, both below the cloud deck and above it to an altitude of at least 120 km (*1*). Below the clouds, the instruments were temperature and pressure sensors and accelerometers; above the clouds, accelerometers alone were used to define the structure from probe deceleration. A goal of the experiment was to measure the structure below the clouds with sufficient accuracy to define the thermal contrast available to drive the circulation.

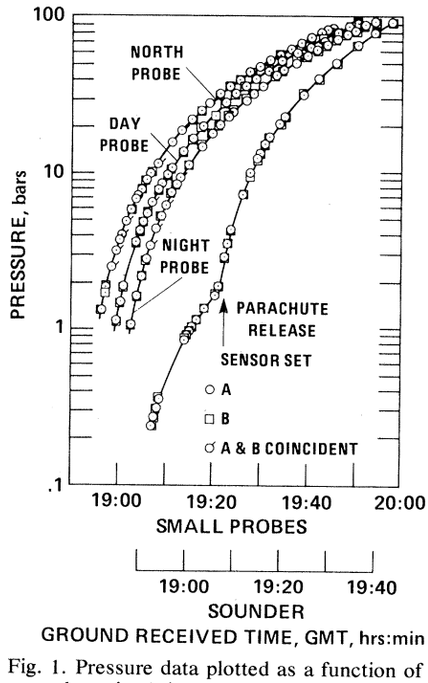

Fig. 1. Pressure data plotted as a function of ground received time. About one-tenth of the points are plotted. The slope discontinuity on the sounder marks the time of parachute release. The more rapid descent of the sounder after it began free fall caused it to land earlier than the three small probes. Its time axis has therefore been displaced. All landed between 19:43 and 19:56 GMT.

In this report we present preliminary results on lower-atmosphere structure, thermal contrasts, and atmospheric stability. We also give altitudes derived from the data and the temperature profile from 67 to 105 km derived from the first analysis of the entry data from the north probe.

In Fig. 1, pressure measurements made during the descent of the four probes are plotted against the time at which the data were received on Earth. Measurements have not yet been fully corrected. The circles and squares in Fig. 1 represent two independent sensor sets on each probe, which generally agree within about 1 percent. The data have been corrected for offset jumps that occurred at pressures above 20 bars, at which the lower range sensor diaphragms burst. Data corrected for the offsets agree well between the two sensor sets on each probe (the corrections for the two sets are independent and the jumps are not simultaneous), and we be-

0036-8075/79/0223-0787$00.50/0